https://doi.org/10.1016/j.seta.2020.100762

Study on the effects of runner geometries on the performance of inline cross-flow turbine used in water pipelines

Jiyun Du[a,b,*], Zhicheng Shen[b], Hongxing Yang[b,*]

[a] Jiangsu Key Laboratory of Advanced Food Manufacturing Equipment & Technology, School of Mechanical Engineering, Jiangnan University, Wuxi 214122, Jiangsu, China

[b] Renewable Energy Research Group (RERG), Department of Building Services Engineering, The Hong Kong Polytechnic University, Hong Kong, China

Corresponding author email: dujiyunupc@hotmail.com; hong-xing.yang@polyu.edu.hk

Abstract

To supply continuous and reliable power to the water monitoring systems and motorized control valves in urban water supply networks, the inline cross-flow turbine has been developed. This study aims to investigate the effects of different runner geometries on the performance of inline cross-flow turbines and to determine the optimal runner geometrical parameters. In this paper, a theoretical analysis of the working mechanism of a cross-flow runner is first performed to study the impacts of the runner geometry on turbine performance. Thereafter, several turbine models with different runner geometries are built and simulated to analyse the output power, water head reduction and torque generation at each runner stage. The results indicate that a good match between the flow inlet angle and blade outer angle notably enhances the turbine performance. Based on the results, the recommended optimal blade outer angle in this research is 30°. In addition, the results also show that the runner diameter ratio has a major impact on torque generation at the runner first stage. A lower runner diameter ratio leads to a higher output power, but the water head reduction is also higher. Based on the results, the suggested runner diameter ratio is 0.68. A numerical study on the number of blades indicates that when the number of blades increases from 20 to 24, the turbine output power considerably rises, and the maximum output power reaches 2285 W. However, if the blade number is further increased, the variation in output power is very slight. Thus, the proposed optimal blade number is 24. Based on the research results, the maximum turbine efficiency can reach 50.9%

after runner optimization.

Keywords: Water pipeline; micro hydropower generation; inline cross-flow turbine; blade outer angle; runner diameter ratio

Nomenclature

D_1	Runner outer diameter (mm)
D_2	Runner inner diameter (mm)
D_2/D_1	Runner diameter ratio
ΔH	Water head reduction through the turbine (m)
N_b	Blade number
P_{in}	Input power of the turbine (W)
P_{out}	Simulated output power of the turbine (W)
P_s	Actual simulation power output (W)
P_{tcft}	Theoretical power of cross-flow turbine (W)
Q	Water flow rate through the turbine (m^3/s)
R_b	Blade radius (mm)
T	Torque of the runner (N·m)
U_x	Velocities of the rotating reference system (m/s)
V_x	Absolute flow velocities (m/s)
V	Average flow velocity at the entrance of first runner stage (m/s)
g	The acceleration of gravity (m/s^2)
r	Runner outer radius (mm)
α_x	Angle between relative flow velocities and velocities of the rotating reference system (°)
β_x	Angle between absolute flow velocities and velocities of the rotating reference system (°)

β_1	Blade outer angle (°)
β_2	Blade inner angle (°)
ρ	Density of water (kg/m^3)
ω	Runner rotation speed (rad/s)
η_{tcft}	Theoretical efficiency of the turbine (%)
η_{me}	Overall mechanical efficiency (%)
η_g	Conversion efficiency of generator (%)
η	Turbine efficiency (%)
TSR	Tip speed ratio

1. Introduction

In many countries and regions worldwide, water monitoring devices, including flow meters and pressure sensors, are widely used for leakage detection along urban water supply pipelines [1]. Usually, these monitoring devices are powered by chemical batteries that only have limited lifespans [2]. Once their batteries approach the end of their service life, these water monitoring systems stop functioning. Therefore, batteries should be replaced regularly, which results in high cost and manpower requirements [3]. Moreover, many motorized control valves powered by underground cables are installed in water supply systems for pressure management and discharge control purposes [4,5]. However, the initial installation cost of underground cables in urban areas is very high, and the installation procedures are relatively complex, which greatly inhibits the wide application of water control valves [6].

Instead of traditional batteries and underground cables, micro hydropower generation in water supply pipelines is a promising power source for water monitoring and control devices [7]. Usually, the water pressure in urban water supply pipes is very high and even in excess to ensure a normal water supply from remote water treatment stations to urban areas; however, in urban water distribution networks, the

water pressure needs to be reduced to avoid water leakage [8,9]. Micro-hydropower technologies generate power using the otherwise dissipated water flow energy, thereby slightly impacting the flow rate and loss across water pipeline pumps.

To harvest the hydropower inside water pipelines, the inline cross-flow turbine that consumes limited water pressure for electricity generation in urban mains has been developed in previous research [10-12]. Fig. 1 shows a prototype of the previously developed inline cross-flow turbine. In the proposed turbine, a part of the water pipeline is selected as the turbine body, and a DN100 T-joint is designed on the turbine body for cross-flow runner insertion. The runner consists of 12 semi-circular blades that are welded onto 3 discs; the runner has no internal shaft, and a runner holder is located on the bottom of the turbine body to hold the runner terminal to reduce runner deformation. A micro-sized 24-V synchronous generator connected to the runner via a shaft is used to transform the torque captured by the runner into electricity. As the installation space is very limited along underground water pipelines, the allocation of the turbine axis is vertical to allow a smaller surface occupation. In this project, the generator is very small; thus, there is a very slight threat to the turbine structural stability. To enhance the turbine performance, two blocks that are welded onto the pipe inner wall are used to guide the water flow towards the blades which generate positive torque after acceleration. The numerical and experimental results have indicated that the developed turbine can very suitably fulfil the power demand of the water monitoring system and motorized control valves [11]. However, more research is still required to investigate the factors influencing the inline turbine performance, which can provide notable guidance for performance enhancement and promote the application of inline cross-flow turbines.

Fig. 1 Prototype of the previously developed inline cross-flow turbine

In previous research, a mathematical design method for the block has been proposed, and the effects of different block parameters, including the orientation angle of the block outlet and runner inlet arc angle, on the turbine performance have been investigated using numerical methods. The optimal block shape has been determined according to the research results [10,12]. Fig. 2 shows a schematic diagram of the inline cross-flow turbine after block optimization. In the inline cross-flow turbine, the conversion block transforms the potential energy of water flow into kinetic energy; thus, the flow velocity towards the runner can be accelerated. In addition, the main function of the guide block is to direct the water flow towards the conversion block and runner. As the cross-flow runner is hollow and water flows transversely through the runner, water passes through the blades passages twice before leaving the runner. Based on the order of water passage, the runner can be divided into two stages: the runner first stage and runner second stage (Fig. 2).

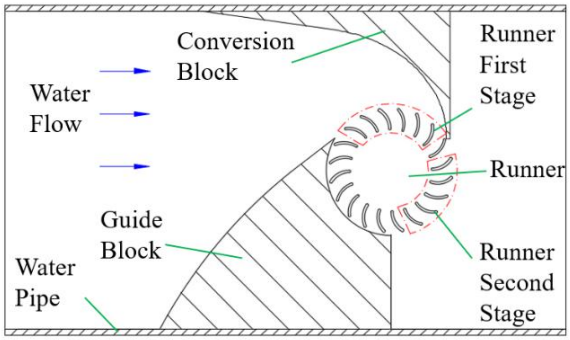

Fig. 2 Schematic diagram of the inline cross-flow turbine

However, according to the results from previous research, mismatching still occurs between the block design and runner design [10], resulting in shock loss and flow separation in the passages between the blades at the runner first stage. To obtain a better design of the cross-flow runner, the present study aims to investigate the impact of runner geometrical parameters on the inline cross-flow turbine performance. Therefore, suitable matching can be achieved between the block design and runner design.

In the current literature, several researchers have investigated the influence of the runner geometry on the performance of traditional cross-flow turbines. The blade outer angle, which represents the inlet angle of the blades at the runner first stage and the outlet angle of the blades at the runner second stage, is one of the key parameters of a cross-flow runner. An unsuitable blade outer angle may cause flow separation and severe hydraulic loss in the blade passages, which adversely impacts the turbine performance. Katayama et al. [13] assessed the performance of four different turbine prototypes whose blade outer angles were 21°, 24°, 27° and 30° by experimental methods and found that the optimal blade outer angle for cross-flow turbines was 30°. Furthermore, numerical studies conducted by Katayama et al. [13] indicated that a suitable blade outer angle can improve the output power ratio of the runner first stage. Choi et al. [14] studied the impact of the blade shape on the performance and inner flow characteristics of cross-flow turbines with the computational fluid dynamics (CFD) method. The results showed that when the attack angle decreases from 35° to 25°, the maximum turbine efficiency increases from 60% to 80%. Elbatran et al. [15] reported that for a dual-nozzle channel cross-flow turbine, the optimal blade outer angle should be 45°. Normally, the widely accepted value for the blade outer angle in the design process of traditional cross-flow turbines is 39° [16].

In addition to the blade outer angle, the blade inner angle also plays an important role in affecting the performance of cross-flow turbines. The blade inner angle is the exit flow angle at the runner first stage and the inlet flow angle at the runner second

stage. In the research of Adhikari [17], the author evaluated the performance of two cross-flow turbines with blade inner angles of 90° and 85° via numerical methods. It was observed that when the blade inner angle was reduced from 90° to 85°, the turbine efficiency decreased from 88% to 83%. As suggested by the literature, 90° is nearly the optimal blade inner angle [18,19]. When the blade inner angle equals 90°, the water flow leaves the runner first stage along the radial direction and enters the runner second stage with a slight energy loss.

Furthermore, the ratio between the runner inner and outer diameters also has an impact on the turbine performance. Aziz and Desai [20] compared the performance levels of cross-flow turbines with ratios of 0.60, 0.68 and 0.75 via the experimental approach and concluded that a diameter ratio of 0.68 is optimal. Adhikari [17] studied the influencing mechanism of the runner diameter ratio on the cross-flow turbine performance via the numerical method. In this research, three models with runner diameter ratios of 0.64, 0.68 and 0.72 were built and simulated. The results indicated that the maximum efficiency of the models with runner diameter ratios of 0.68 and 0.72 was 88% and 83%, respectively; however, when the ratio was reduced from 0.68 to 0.64, the efficiency difference was very slight.

In the research of Sammartano et al. [18], a two-step design procedure was proposed for the nozzle design and runner parameter optimization of traditional cross-flow turbines. Hence, a new type of inline cross-flow turbine for either discharge regulation or pressure control was designed based on the above design procedure [21,22]. An experimental study indicated that the efficiency of the proposed inline cross-flow turbine can reach 76% [23]. However, due to the wide range of possible working conditions, a standard design criterion for cross-flow turbines has yet to be established [18]. In previous research, a theoretical design method for the ducted elements of inline cross-flow turbines has been proposed, and the optimal design of the ducted elements has been obtained [10-12]. Although the optimal geometrical parameters of cross-flow runners have been suggested by many

investigators, there has been no research on determining the best runner geometry for cross-flow turbines that are used in water pipelines. Therefore, in the present paper, the influence of different runner geometries on the performance of inline cross-flow turbines is studied by the CFD method, and the optimal runner geometrical parameters are determined. The rest of the paper is organized as follows: Section 2 presents the theoretical analysis on the working mechanism of the cross-flow runner. Section 3 describes the numerical and experimental methodologies used in this research. Section 4 presents the numerical results and corresponding analysis. Finally, the Conclusion section summarizes the main findings and conclusions.

2. Theoretical analysis on the cross-flow runner

The runner is one of the most important components of cross-flow turbines because it captures the torque from water flow and then transmits it to the generator. Theoretical analysis of its working mechanism can offer inspiration for its geometrical improvement. In this part, the expression of the turbine efficiency is derived based on Euler's equation for rotating machines; thus, the influencing factors of the turbine performance can be analysed. Finally, the main geometrical parameters of the blades are introduced.

2.1 Expression of the inline cross-flow turbine efficiency

Fig. 3 shows the steady flow through a cross-flow runner. The unique characteristic of a cross-flow turbine indicate that water flows through the blade passages twice before leaving the runner. Therefore, the theoretical power of the cross-flow turbine is composed of two parts: power from the runner first stage and from the runner second stage.

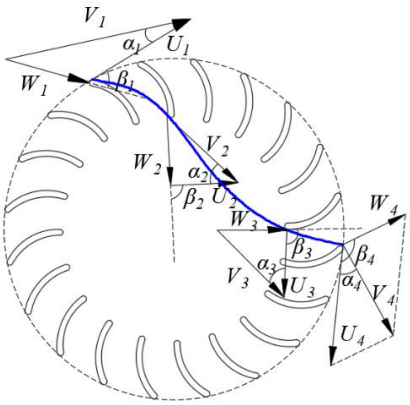

Fig. 3 Flow streamline through the cross-flow runner

Based on Euler's equation for rotating machines [18], the theoretical output power of cross-flow turbine can be calculated by:

$$P_{tcft} = Q\rho(V_1U_1\cos\alpha_1 - V_2U_2\cos\alpha_2 + V_3U_3\cos\alpha_3 - V_4U_4\cos\alpha_4) \tag{1}$$

It is assumed that there no energy loss occurs in the space between the first and second stages. Based on Fig. 3, the following equations can be obtained:

$$V_2 = V_3 \tag{2}$$

$$U_2 = U_3 = \frac{D_2}{2}\omega \tag{3}$$

$$\alpha_2 = \alpha_3 \tag{4}$$

Eq. 1 can be modified as:

$$P_{tcft} = Q\rho U_1(V_1\cos\alpha_1 - V_4\cos\alpha_4) \tag{5}$$

Based on the flow velocity triangles at the runner inlet and outlet:

$$V_1\cos\alpha_1 = U_1 + W_1\cos\beta_1 \tag{6}$$

$$V_4\cos\alpha_4 = U_4 + W_4\cos\beta_4 \tag{7}$$

$$\beta_4 = 180^\circ - \beta_1 \tag{8}$$

$$U_1 = U_4 = \frac{D_1}{2}\omega \tag{9}$$

Eq. 1 can be further modified as:

$$P_{tcft} = 2Q\rho U_1\left(V_1\cos\alpha_1 - U_1\right) \tag{10}$$

The input power can be calculated:

$$P_{in} = \rho g Q \Delta H = \rho Q V_1^2/2 \tag{11}$$

Hence, the theoretical efficiency can be obtained as:

$$\eta_{tcft} = P_{tcft}/P_{in} = 4\frac{U_1}{V_1}\cos\alpha_1 - 4\left(\frac{U_1}{V_1}\right)^2 \tag{12}$$

Referring to Eq. 12, the efficiency of inline cross-flow turbines depends on variables $\frac{U_1}{V_1}$ and α_1. Here, $\frac{U_1}{V_1}$ is determined by the block shape [10,12], while α_1 is determined by the blade outer angle. Therefore, the theoretical analysis of the working mechanism of the cross-flow runner indicates that the blade outer angle is of vital importance for the performance enhancement of inline cross-flow turbines.

2.2 Main geometrical parameters of the blades

Fig. 4 shows the key blade geometries of the cross-flow turbine, including the outer blade angle β_1, inner blade angle β_2 and blade radius R_b. Among them, the optimal values of β_1 and β_2 can be determined based on simulation results. The blade radius R_b can be calculated by [17]:

$$R_b = \frac{D_1^2 - D_2^2}{4D_1\cos\beta_1} \tag{13}$$

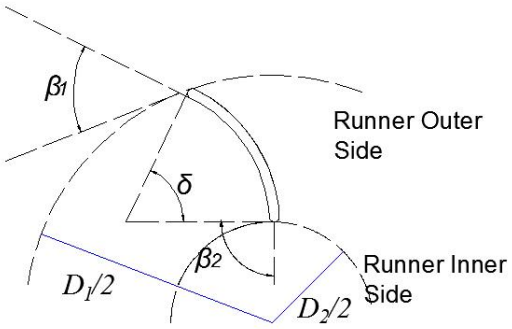

Fig. 4 Blade shape of the cross-flow runner

It can be observed from the above equation that the blade shape can not only be affected by the blade outer angle but can also be controlled by the runner inner and outer diameters, which means that after determination of β_1 and D_1, the runner diameter ratio D_2/D_1 will also influence the blade shape. Therefore, it is also very important to investigate the impact of D_2/D_1 on the turbine performance to determine the optimal diameter ratio.

Moreover, the blade thickness also plays an important role in affecting the hydraulic performance of inline cross-flow turbines. Specifically, the turbine performance increases with decreasing blade thickness; however, as the blades are subjected to cyclic loading, the blade thickness must be sufficient to resist water thrust and fatigue [23]. In this research, the blade thickness is set to 2 mm, which has been proven reliable and durable in our previous field tests [11].

3. Research methodology

3.1 Numerical approach

For hydro-turbine or wind turbine development and optimization, the CFD method has been proven to be a promising technique [24,25]. In this paper, the CFD method is adopted to provide an in-depth understanding of the influence of the different runner geometries on the performance of inline cross-flow turbines.

3.1.1 Grid generation

Various 3D inline cross-flow turbine models were established in SolidWorks 2014 and then imported into ANSYS ICEM for meshing (Fig. 5). As the turbine model is symmetrical, only one symmetric part was modelled and simulated, assuming an impermeable boundary along the symmetry plane. The computational model of the inline cross-flow turbine was composed of a turbine body and runner. To reduce the uncertainty of numerical computation, models of two extension parts were built upstream and downstream of the turbine. In the computational model of the inline cross-flow turbine, the runner was considered the rotating domain, and the other parts were regarded as the stationary domain. The whole computational domain was discretized using unstructured grids to obtain a good balance between the calculation time and accuracy, and prism grids were adopted to discretize the domains near the boundaries, i.e., the blade walls, while tetra grids were utilized for grid generation far from the boundaries.

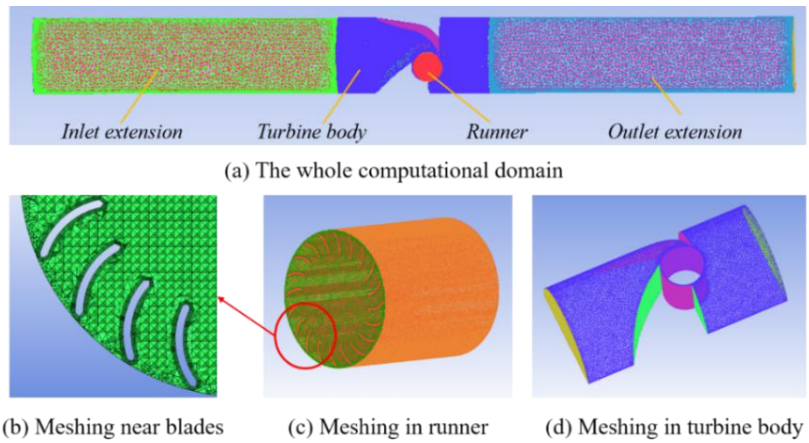

Fig. 5 The meshing of the computation domain

Usually, grid independence tests are conducted in the meshing process to reduce the calculation uncertainty as well as to minimize the computation time. In this study, different meshing schemes with grid numbers of 1.8, 2.9, 3.8 and 5.3 million were realized and tested. Fig. 6 shows the grid independence test results. It can be concluded that a grid number of approximately 3.8 million is the ideal value for the

following studies.

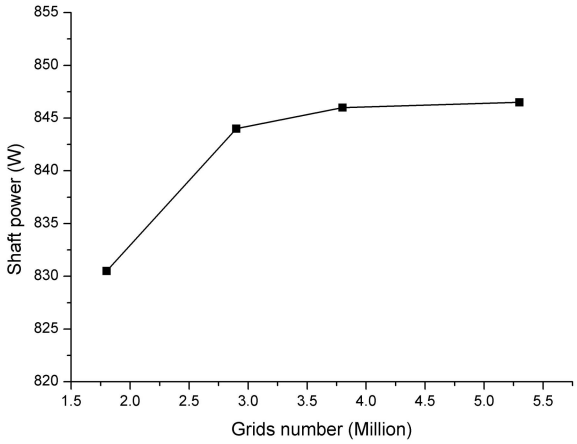

Fig. 6 Grid independence test results

3.1.2 Numerical setup

The numerical simulations were conducted in ANSYS CFX by adopting the SST $k-\omega$ turbulence model, which has been demonstrated to be a relatively accurate model for numerical hydro-turbine simulations by several researchers [17,26,27]. The advection scheme was selected at a high resolution, while the target RMS was set to 10^{-5}. According to the real conditions in urban water pipelines, the inlet and outlet boundary conditions were then determined. The detailed boundary conditions in the simulation setup are listed in Table 1.

Table 1 Boundary conditions of the whole computation domain

Boundary conditions	Setup
Inlet	Flow velocity: 1.5 m/s
Outlet	Atmospheric pressure
Blades and pipe wall	Non-slip smooth wall
Symmetry plane	Impermeable boundary

3.2 Experimental setup

In the research process, a hydraulic test rig (as shown in Fig. 7) was built in a

laboratory at the Hong Kong Polytechnic University. The test rig consisted of two centrifugal pumps, a water tank, an electromagnetic flow meter, two pressure sensors, a ball valve and a controller system including a controller and two 12-V/17-Ah lead-acid batteries in series. In addition, a frequency converter controller was used to control the working flow rate and pressure of the centrifugal pumps. Generally, the flow velocity range in the test rig was 1.0-3.0 m/s, and the maximum water pressure reached 40 m. The water head reduction was measured by the pressure sensors, and the flow velocity in the pipes was detected by the electromagnetic flow meter. In the described test rig, the precision of the flow meter and pressure sensors were ±0.5% full scale and ±0.25% full scale, respectively. Based on prescribed methods for uncertainty estimation [28], the composite measurement error of the water head was ±0.25%, while that of the turbine efficiency was ±0.56%.

In this research, a micro-sized 24-V synchronous generator is used to transform the rotation of the turbine shaft into electricity. As the micro-sized inline hydropower harvesting system is a stand-alone system without a connection to the electric network and large discharge variations usually occur in real water pipelines, a power management and storage system consisting of a controller and two batteries (Fig. 7) has been developed. The power from the generator is stored in the batteries after rectification of the controller. In addition, when the flow rate is too high, the controller will cut off the power input to protect the circuits and batteries; when the flow rate is too low, the batteries will continue to supply power to the water monitoring system and motorized control valves.

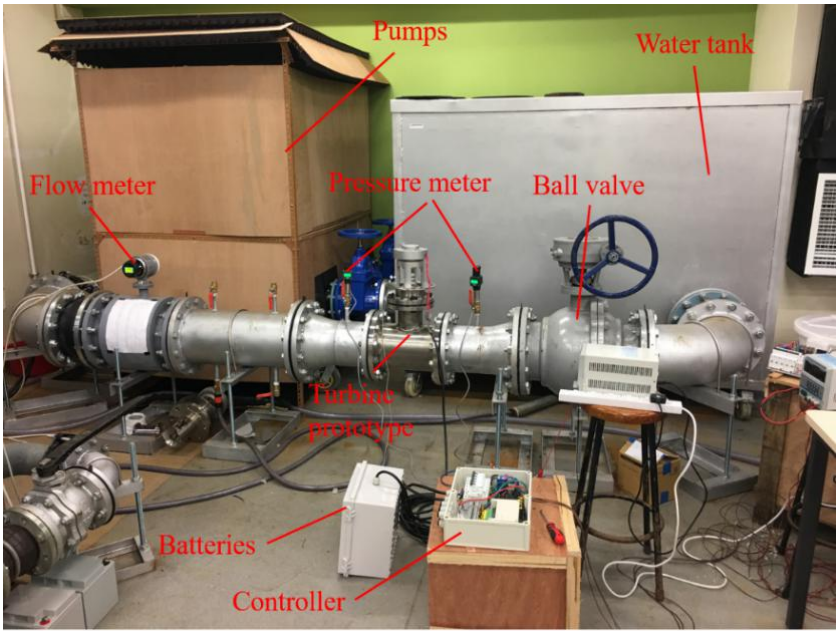

Fig. 7 The hydraulic test rig

3.3 Data analysis

To better assess the turbine performance under the different runner designs, the tip speed ratio (TSR), which is expressed by Eq.14, is introduced.

$$TSR = \frac{r\omega}{V} \tag{14}$$

In this research, V is regarded as uniform. Thus, by varying the values of ω in the simulation solver setup, the turbine performance at different TSRs can be obtained.

This study numerically investigates the effects of different runner geometries on the inline cross-flow turbine performance. Therefore, it is critical to validate the numerical method by comparing the experimental and numerical results. In the CFD simulations, only the output torque of the runner can be recorded. However, in the experiments, the power produced by the generator is recorded for turbine performance assessment. Therefore, to compare the experimental and numerical results, the simulation data need to be processed with the following equations [32]:

$$P_{out} = \eta_{me}\eta_g T\omega \tag{15}$$

$$P_{in} = \rho g \Delta H Q \tag{16}$$

$$\eta = \frac{P_{out}}{P_{in}} \tag{17}$$

4. Results and analysis

4.1 Validation of the numerical method

In this research, the numerical method is validated by the experimental results obtained by testing the turbine prototype on the test rig described above. Fig. 8 shows the output power obtained by the numerical and experimental methods, while Table 2 compares the detailed values and their relative errors at different flow velocities. Regardless of the errors between the experimental and numerical results at high flow velocities (1.7-2.0 m/s), the numerical results present a similar trend with that of the experimental results.

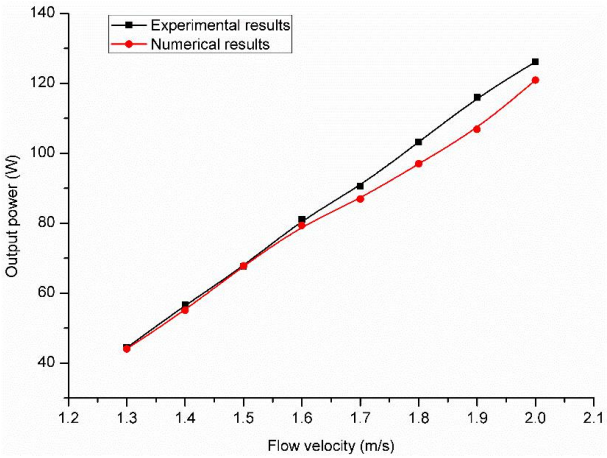

Fig. 8 Validation of the numerical method

Table 2 Numerical and experimental output power and relative errors

Flow velocity (m/s)	Experimental output power (W)	Numerical output power (W)	Error (%)
1.3	44.4	44.0	-0.9
1.4	56.6	55.1	-2.6
1.5	67.6	67.8	0.3
1.6	81.1	79.4	-2.1
1.7	90.6	86.9	-4.1
1.8	103.2	97.0	-6.0
1.9	116	106.8	-7.9
2.0	126.2	121.0	-4.1

Two main reasons may account for the deviations between the experimental and numerical results. On the one hand, the computational model is simplified, resulting in unavoidable calculation uncertainties. On the other hand, in the experimental process, measuring errors are very difficult to eliminate and also influence the accuracy of the experimental results. Table 2 indicates that the maximum error percentages are no larger than 8%, and the error value at a water velocity of 1.5 m/s is only 0.3%. The present research mainly focuses on the turbine performance under the given design conditions (a working flow velocity 1.5 m/s); therefore, the described numerical method is accurate enough for the performance prediction of the inline cross-flow turbines in this research [29-31].

4.2 Study on the effects of the blade outer angle

4.2.1 The optimal range of the blade outer angle

When the cross-flow turbine is in operation, water flows through the blades passages twice. Based on Fig. 3, at the runner first stage, the blade outer angle is the blade inlet angle. However, the latter becomes the blade outlet angle at the runner second stage. Several optimal blade outer angles have been suggested by many

researchers using either numerical or experimental methods; however, due to the different applications, the blade outer angles of cross-flow turbines are rarely uniform [18]. Fig. 9 shows the distribution of the flow inlet angle along the runner inlet arc from the simulation results of the turbine model, which has the optimal block design [10]. The flow attack angle decreases when the runner inlet arc angle increases from 0° to 50° and fluctuates between 26° and 32° in the runner inlet arc angle range from 50° to 105°. This phenomenon mainly occurs because at the beginning of the runner inlet (from 0° to 50°), the conversion block cannot fully control the inlet angle of the water flow, and along the runner inlet, the functionality of the conversion block gradually increases. Moreover, the inlet velocity fluctuation is mainly caused by interference of the blades.

It can be speculated that the blade outer angle, which could achieve a good matching with the flow inlet angle, may range from 26° to 32°. In this part of the research, CFD simulations were performed with β_1 values of 26°, 28°, 30° and 32°. The block geometries determined in previous research are selected as the optimal geometries [10,12], and the main geometrical parameters of the studied runner are listed in Table 3.

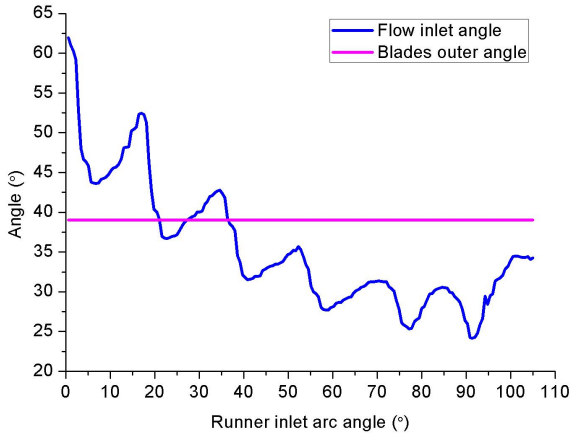

Fig. 9 The distribution of the flow inlet angle along the inlet arc of the runner

Table 3 The main runner geometries of the turbines for the different β_1 values

Blade outer angle β_1	Blade inner angle β_2	Runner diameter ratio D_2/D_1	Blade radius R_b	Blade number N_b
26°	90°	0.68	14.9 mm	20
28°	90°	0.68	15.2 mm	20
30°	90°	0.68	15.5 mm	20
32°	90°	0.68	15.8 mm	20

4.2.2 Turbine performance at the different blade outer angles

In the simulation cases, the flow velocity was set to 1.5 m/s, and the turbine performance was studied at the different TSRs. The simulated output power, water head reduction and efficiency of the turbine are shown in Fig. 10. Fig. 10(a) shows that when the blade outer angle is 28° or 30°, the turbine has a higher output power than that of the other cases. Moreover, when the TSR is 1.2 and the blade outer angle equals 30°, the output power reaches 2200 W, which is the maximum value among the simulation results. In addition, it is interesting to observe that in Fig. 10(a), with increasing TSR, the output power deviation between the different models becomes more notable. This mainly occurs because at higher TSRs, the hydraulic and shock losses at the runner inlet are more severe and more energy is wasted.

Fig. 10(b) indicates that the water head reduction through the turbine increases slightly when β_1 increases from 26° to 32°. The turbine with β_1=26° consumes a larger water head than the other turbine models. The main reason for this finding is that severe hydraulic and shock losses may occur in the blade passages of the turbine model at β_1=26° because the blade outer angle does not match the flow inlet angle very well. In terms of the turbine efficiency, Fig. 10(c) shows that with increasing blade outer angle, the best turbine efficiency gradually increases until reaching its maximum value and then decreases. In this process, the maximum best turbine

efficiency is 49.6% when the blade outer angle is 30°. It can be concluded from the results shown in Fig. 10 that the blade outer angle has a major impact on the hydraulic losses at the runner inlet, thus affecting the turbine performance. It is of vital importance to achieve a suitable matching between the inlet flow and runner geometry by selecting an appropriate blade outer angle. Based on the results and analysis, it is suggested that the best blade outer angle of the developed inline cross-flow turbine is 30°.

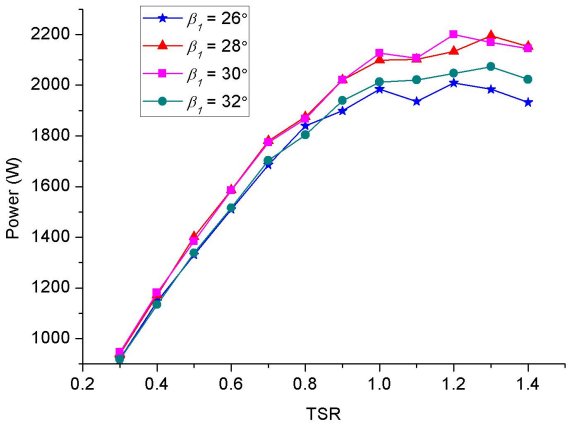

(a)

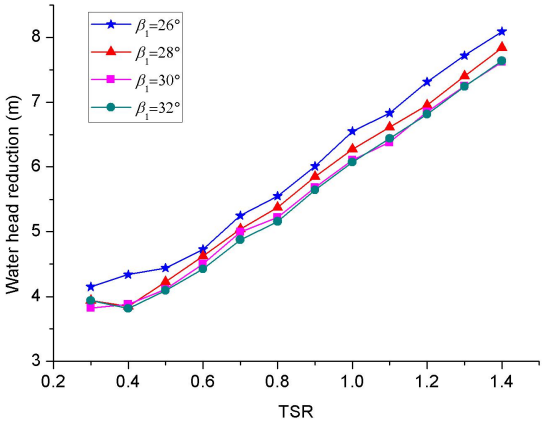

(b)

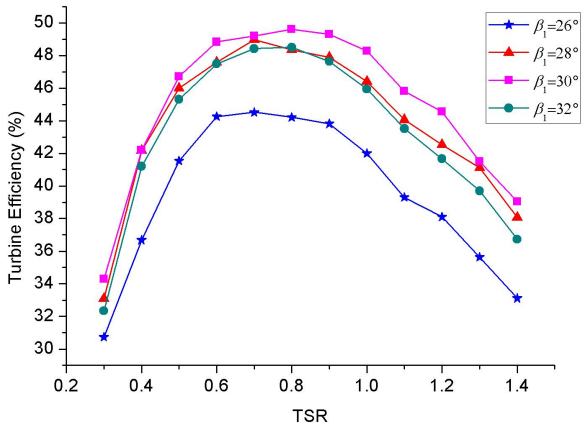

(c)

Fig. 10 The influence of the blade outer angle on the (a) turbine output power, (b) water head reduction, and (c) turbine efficiency

4.2.3 Torque output of each runner stage

Fig. 11 shows a comparison of the torque output of each blade in the turbine models for the different blade outer angles. It is clear that at the first runner stage, the torque generated by each blade increases along the runner inlet arc towards the runner second stage. The main reason for this phenomenon is that along the runner inlet arc, the function of the conversion block becomes more apparent, and an increasing water head is converted into water flow kinetic energy; thus, more energy is captured by the blades at the end of the runner inlet arc. Moreover, it is observed that in the turbine model with a blade outer angle of 30°, the blades at the runner first stage attain a higher performance in terms of the torque output. This mainly occurs because in this model, the flow inlet angle better matches the blade outer angle; thus, water flows along the blades more smoothly with lower hydraulic losses. This phenomenon is also in correspondence with the results presented in the above chapter. In addition, at the runner second stage, the blades in the middle generate more torque because more water flows through these blades.

Furthermore, the proportion of the overall torque output of each runner stage in the four turbine models is compared in Fig. 12. As is evident, the first and second

runner stages generate nearly the same torque in all cases, which means that each runner stage generates almost 50% of the total torque. However, the torques produced by each stage in the models are slightly different, which results from the variation in the blade outer angle. Among the four studied models, the one with β_1=30° generates the most torque at the runner first stage. This result further illustrates that if the flow inlet angle can be suitably matched with the blade outer angle, the performance of the runner first stage can be improved as the hydraulic and shock losses in the blade passages are reduced.

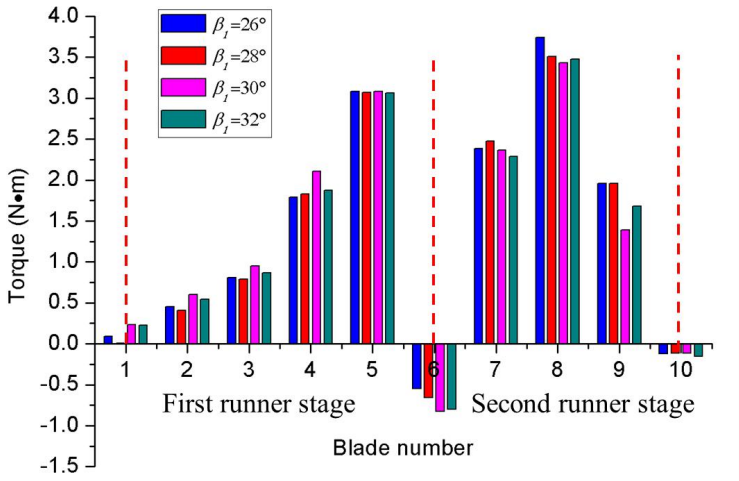

Fig. 11 Torque output of each blade in the different turbine models

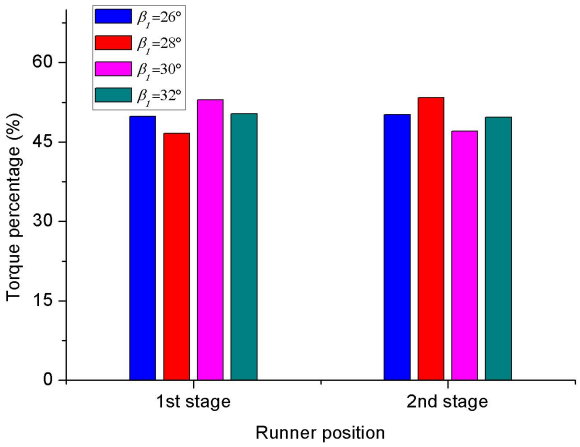

Fig. 12 Torque output of each runner stage in the different turbine models

4.3 Study on the effects of the runner diameter ratio

The ratio between the runner inner and outer diameters (D_2/D_1) can influence the blade radius and can further affect the curvature and length of each blade [17]. For the different runner diameter ratios, the blade passage and length are different, resulting in different hydraulic and friction losses. The variation in the runner diameter ratio also influences the torque capture from water flow due to the different blade lengths. Based on the literature review, the suggested runner diameter ratio is 0.68 in previous studies. However, as there has been no relevant research on the effects of the diameter ratio on the performance of inline cross-flow turbines, it is necessary to determine the optimal D_2/D_1 ratio for this custom application. In the present research, three models with D_2/D_1 ratios of 0.64, 0.68 and 0.72 are established and simulated. In the simulation process, the block parameters suggested in the previous parts are selected as the optimal values, and the main geometrical parameters of the runner are summarized in Table 4.

Table 4 The main runner geometrical parameters for the different D_2/D_1 ratios

Runner diameter ratio D_2/D_1	Blade outer angle β_1	Blade inner angle β_2	Blade radius R_b	Blade number N_b
0.64	30°	90°	16.7 mm	20
0.68	30°	90°	15.5 mm	20
0.72	30°	90°	13.6 mm	20

4.3.1 Turbine performance at the different diameter ratios

Fig. 13(a) shows the influence of the runner diameter ratio on the turbine output power. It shows that when D_2/D_1 increases from 0.68 to 0.72, the turbine output power considerably decreases. As shown in Fig. 13(b), the water head reduction caused by the turbine application also slightly decreases with D_2/D_1 increasing from 0.68 to 0.72. The main reason for these variations is that when D_2/D_1 increases, the blade length decreases. Therefore, the blades have fewer opportunities to capture torque from the

water flow, and less kinetic energy is transferred from the water flow to the runner. The turbine efficiency is much lower than that of the other models when D_2/D_1 is 0.72; specifically, the maximum turbine efficiency decreases from 49.6% to 47.2% when D_2/D_1 increases from 0.68 to 0.72. It is worth noting that both the output power and water head reduction notably increase when the runner diameter ratio decreases from 0.68 to 0.64. The main reason for the increase in output power is that with decreasing diameter ratio, the blade length increases, and the blades have more opportunities to capture kinetic energy from the water flow. However, when the diameter ratio decreases, the blade curvature also decreases, and the external profile of the blades changes, which may result in flow separation near the blade surface and cause a hydraulic loss in the blade passages. Fig. 13(c) shows the influence of the runner diameter ratio on the turbine efficiency. The maximum turbine efficiencies when D_2/D_1 is equal to 0.68 and 0.64 are 49.6% and 49.8%, respectively. When the TSR is lower than 0.8, the efficiency of the turbine at D_2/D_1=0.68 is higher than that of the turbine at D_2/D_1=0.64. A turbine model with a lower runner diameter ratio causes less water head reduction but also generates less power. Considering the water head reduction and turbine efficiency simultaneously, the suggested runner diameter ratio in this research is 0.68.

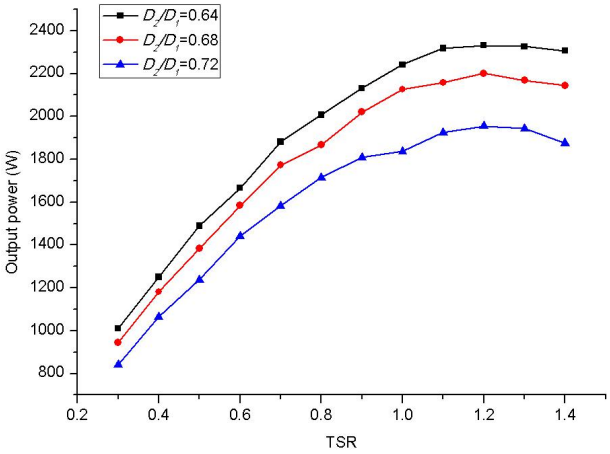

(a)

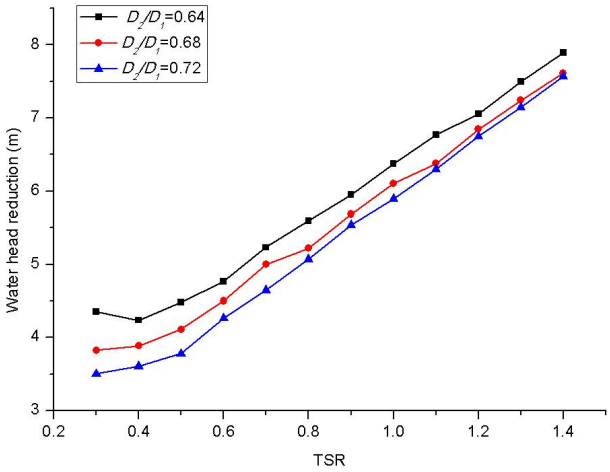

(b)

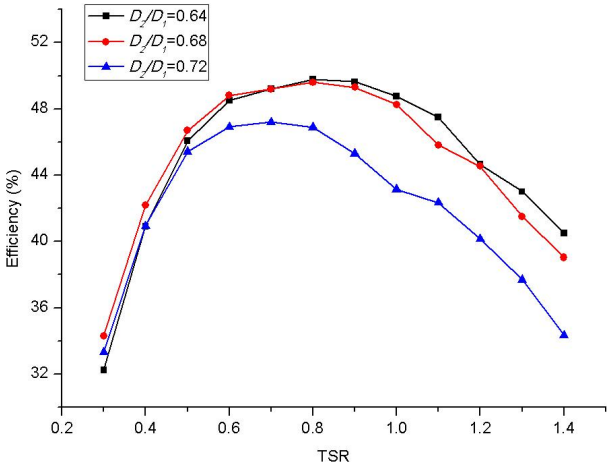

(c)

Fig. 13 The influence of the runner diameter ratio on the (a) turbine output power, (b) water head reduction, and (c) turbine efficiency

4.3.2 Torque output of each runner stage

Figs. 14 and 15 show the influence of the runner diameter ratio on the torque output of each blade and runner stage. As shown in Fig. 14, when D_2/D_1=0.64, the torque output generated by the first runner stage is the highest, while the lowest torque output from the first runner stage occurs when D_2/D_1=0.72. The key reason for this phenomenon is the larger blade length and smaller blade curvature when D_2/D_1=0.64. In contrast, when D_2/D_1=0.72, the torque output from the first runner stage is the lowest due to the smaller blade length and larger blade curvature. As shown in Fig. 14, when D_2/D_1=0.64, the torque generated by the second runner stage

is also the highest. Fig. 15 reveals the influence of the runner diameter ratio on the torque output of each runner stage. The torque percentage of each runner stage is similar when D_2/D_1 equals 0.64 and 0.68, and the first runner stage generates more torque than the second runner stage in these two models. The torque output of the first runner stage is low when D_2/D_1=0.72, and the torque percentage of the second runner stage is much higher than that of the first runner stage in this model. This mainly occurs because in the model at D_2/D_1=0.72, the water flow still has a sufficient kinetic energy when entering the runner second stage, as the blades at the runner first stage have fewer opportunities to capture energy from the water flow.

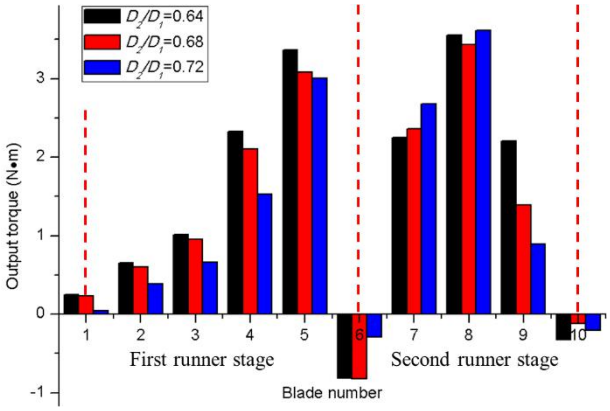

Fig. 14 The influence of the runner diameter ratio on the torque output of each blade

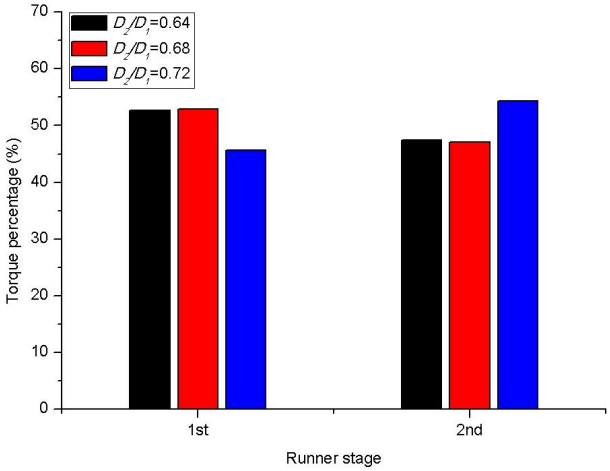

Fig. 15 The influence of the runner diameter ratio on the torque output of each runner

4.4 Study on the effects of the blade number

4.4.1 Turbine performance under the different blade numbers

The blade number (N_b) is another parameter that may influence the turbine performance by affecting the flow separation in the blade passages and the power extraction of each runner stage. In this study, three turbine models with blade numbers of 20, 24 and 28 were built and simulated. Fig. 16 shows the influences of the number of blades on the output power, water head reduction and efficiency of the inline cross-flow turbine. When the blade number increases from 20 to 24, the turbine output power drastically rises, and the maximum output power reaches 2285 W. However, if the blade number is further increased, the variation in output power is very slight. In terms of the water head reduction, the difference between the three investigated models is very slight. The water head reduction of all three models increases with increasing TSR, but the model with more blades consumes a larger water head, which mainly occurs because a runner with more blades has more opportunities to capture kinetic energy from the water flow; thus, a higher potential energy is consumed through the turbine model with more blades. Moreover, a larger blade number means narrower blade passages between the blades; thus, the friction loss may be higher in the models with the larger blade numbers.

Based on Fig. 16(c), the three models have a similar efficiency at a TSR below 0.7; however, the efficiency of the turbine model with a blade number equal to 20 is much lower than that of the other two models at higher TSRs. For all three models, the turbine efficiency increases with increasing TSR until reaching the maximum efficiency, after which the turbine efficiency decreases. The TSR resulting in the highest model efficiency is 0.8. The recorded maximum efficiency is 50.9% when N_b =24. In conclusion, the optimal blade number for the inline cross-flow turbine is 24. However, it is suggested to determine the number of blades according to the mechanical processing level, as the processing time of a runner with more blades is

relatively long and the processing cost could be very high.

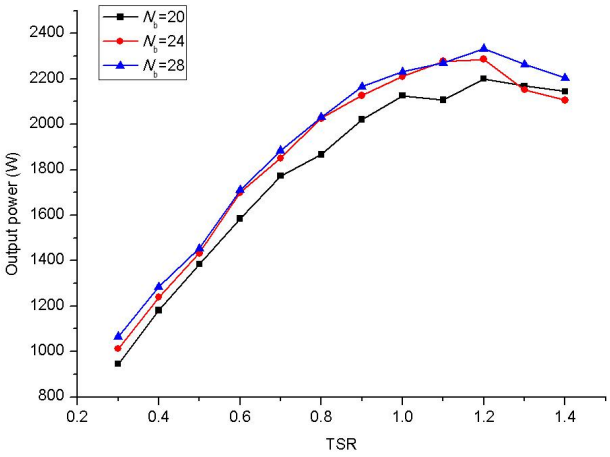

(a)

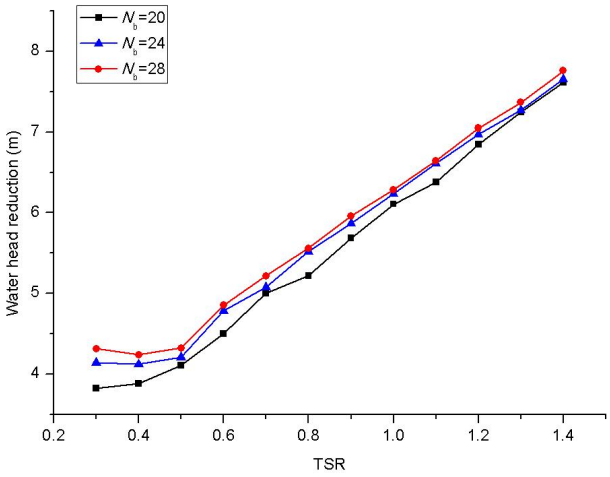

(b)

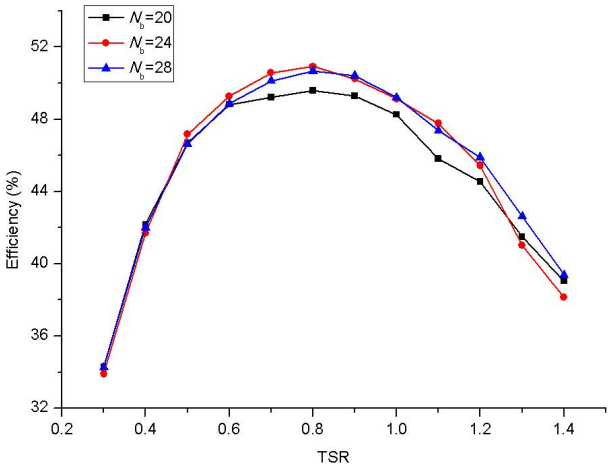

(c)

Fig. 16 The influence of the blade number on the (a) turbine output power, (b) water

head reduction, and (c) turbine efficiency

4.4.2 Torque output of each runner stage

The torque output of each runner stage is shown in Fig. 17. It can be observed that with increasing number of blades, the torque output from the second runner stage increases. This mainly occurs because when the blade number increases, the opportunity of extracting power at the second stage is improved as the blade inlet angle varies considerably at the second stage; thus, the mismatch between the flow inlet and blade inlet angles can be reduced at the runner second stage, and the hydraulic losses also decrease [17]. However, a larger blade number shrinks the blade passages, resulting in turbine efficiency reduction. In addition, the friction loss will also increase with increasing blade number.

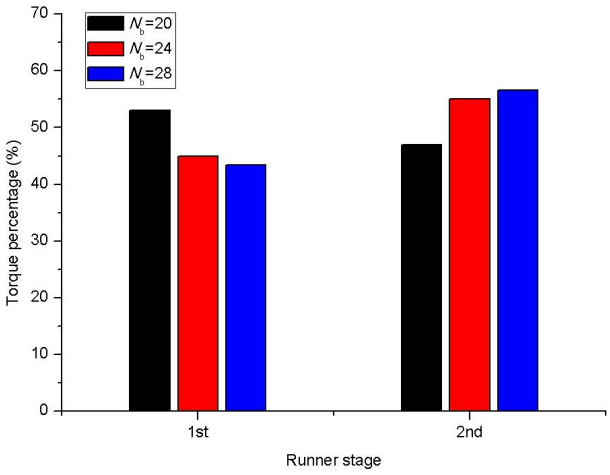

Fig. 17 The influence of the number of blades on the torque output of each runner stage

5. Conclusions

In this paper, the influence of various runner and blade geometrical parameters, including the blade outer angle, runner diameter ratio and blade number, on the performance of inline cross-flow turbines has been numerically investigated. The present research not only reveals the affecting mechanism of the runner and blade geometries on the turbine performance but also suggests optimal values of the runner

and blade geometrical parameters for inline cross-flow turbine applications. The main conclusions from this study are as follows:

(1) By achieving a better matching between the flow inlet angle and blade outer angle in the inline cross-flow turbine, the turbine performance can be greatly enhanced. Specifically, the highest efficiency of the developed turbine can reach as high as 49.6% by improving the blade outer angle. Furthermore, a suitable blade outer angle can significantly improve the torque generated by the runner first stage. Based on the numerical results, the blade outer angle of the inline cross-flow turbine is suggested to be 30°.

(2) The numerical study indicates that a lower runner diameter ratio may lead to a higher output power, but the water head reduction also increases. The runner diameter ratio affects the turbine performance mainly by influencing the performance of the first runner stage. Based on the results, the suggested runner diameter ratio is 0.68.

(3) The investigation of the blade number indicates that when the blade number increases from 20 to 24, the turbine output power substantially rises, and the maximum output power reaches 2285 W. However, if the blade number is further increased, the variation in output power is very slight. The variation in water head reduction with increasing blade number is very slight. The optimal blade number is suggested to be 24, and the recorded maximum efficiency is 50.9% at a TSR of 0.8.

(4) The maximum efficiency of the developed inline cross-turbine is still lower than that of the turbine introduced in Ref. [23]. This phenomenon could be the result of the design of the diffusor. In the present design, the length of the diffusor is smaller to allow a smaller length of the entire device, and the profile of the diffusor has not been specially designed. Therefore, it is suggested to develop a design and optimization method for the diffusor in future research to further

enhance the turbine performance.

Acknowledgement

The authors would appreciate the financial supports provided by the Innovation and Technology Fund of the Hong Kong Special Administrative Region Government (Grant No.: ITS/032/13), the Fundamental Research Funds for the Central Universities (Grant No.: JUSRP12034) and the support from the Water Supplies Department of the Hong Kong SAR Government.

References

[1] Lunqiang Ye. Study on embedded system in monitoring of intelligent city pipeline network (2020). Computer Communications, 153:451-458.

[2] Cadini, F., Sbarufatti, C., Cancelliere, F., & Giglio, M. (2019). State-of-life prognosis and diagnosis of lithium-ion batteries by data-driven particle filters. Applied Energy, 235, 661-672.

[3] Valera, A. C., Soh, W. S., & Tan, H. P. (2017). Enabling sustainable bulk transfer in environmentally-powered wireless sensor networks. Ad Hoc Networks, 54, 85-98.

[4] Paola, F. D., Giugni, M., & Portolano, D. (2017). Pressure management through optimal location and setting of valves in water distribution networks using a music-inspired approach. Water Resources Management, 1-17.

[5] Nazif, S., Karamouz, M., Tabesh, M., & Moridi, A. (2010). Pressure management model for urban water distribution networks. Water Resources Management, 24(3), 437-458.

[6] Zarchi, D. A., & Vahidi, B. (2018). Multi Objective Self Adaptive Optimization Method to Maximize Ampacity and Minimize Cost of Underground Cables. Journal of Computational Design and Engineering, 5(4), 401-408.

[7] Coelho, Bernardete, Andrade-Campos, & Antonio. (2018). Energy recovery in water networks: numerical decision support tool for optimal site and selection of micro turbines. Journal of Water Resources Planning & Management, 144(3), 04018004.

[8] Nourhan Samir, Rawya Kansoh, Walid Elbarki, Amr Fleifle. (2017). Pressure control for minimizing leakage in water distribution systems. Alexandria Engineering Journal, 56(4), 601-612.

[9] Giacomo Galuppini, Enrico Creaco, Chiara Toffanin, Lalo Magni. (2019). Service pressure regulation in water distribution networks. Control Engineering Practice, 86, 70-84.

[10] DU, Jiyun; SHEN, Zhicheng; YANG, Hongxing. Effects of different block designs on the performance of inline cross-flow turbines in urban water mains. Applied energy, 2018, 228: 97-107.

[11] Du, J., Yang, H., Shen, Z., & Guo, X. (2018). Development of an inline vertical cross-flow turbine for hydropower harvesting in urban water supply pipes. Renewable Energy, 127, 386-397.

[12] Du, J., Shen, Z., & Yang, H. (2018). Numerical study on the impact of runner inlet arc angle on the performance of inline cross-flow turbine used in urban water mains. Energy, 158, 228-237.

[13] Katayama, Y., Iio, S., Veerapun, S., & Uchiyama, T. (2015). Investigation of blade angle of an open cross-flow runner. International Journal of Turbo & Jet-Engines, 32(1), 65-72.

[14] Choi, Y. D., Lim, J. I., Kim, Y. T., & Lee, Y. H. (2008). Performance and internal flow characteristics of a cross-flow hydro turbine by the shapes of nozzle and runner blade. Journal of fluid science and technology, 3(3), 398-409.

[15] A. H. Elbatran, O. B. Yaakob, Y. M. Ahmed, A. S. Shehata. (2018). Numerical and experimental investigations on efficient design and performance of hydrokinetic Banki cross flow turbine for rural areas. Ocean Engineering, 159, 437-456.
[16] Adhikari, R., & Wood, D. (2018). The Design of High Efficiency Crossflow Hydro Turbines: A Review and Extension. Energies, 11(2), 267.
[17] Adhikari R. Design Improvement of Cross-flow Hydro Turbine[D]. University of Calgary, 2016.
[18] Sammartano V, Aricò C, Carravetta A, et al. Banki-Michell optimal design by computational fluid dynamics testing and hydrodynamic analysis. Energies, 2013, 6(5): 2362-2385.
[19] R. C. Adhikari, D. H. Wood. (2018). Computational analysis of part-load flow control for crossflow hydro-turbines. Energy for Sustainable Development, 45, 38-45.
[20] Aziz, N. M., & Desai, V. R. (1991). An Experimental Study of the Effect of Some Design Parameters in Cross-Flow Turbine Efficiency. Engineering Report, Department of Civil Engineering, Clemson University.
[21] Sinagra, M., Sammartano, V., Morreale, G., Tucciarelli, T. (2017). A new device for pressure control and energy recovery in water distribution networks. Water, 9(5), 309.
[22] Sammartano, V., Sinagra, M., Filianoti, P., Tucciarelli, T. (2017). A Banki-Michell turbine for in-line hydropower systems, Journal of Hydraulic Research, 55 (5) ,686-694.
[23] Sinagra, M., Aricò, C., Tucciarelli, T., Morreale, G. (2020). Experimental and numerical analysis of a backpressure Banki inline turbine for pressure regulation and energy production. Renewable Energy, 149, 980-986.
[24] Chong, W. T., Muzammil, W. K., Wong, K. H., Wang, C. T., Gwani, M., Chu, Y. J., & Poh, S. C. (2017). Cross axis wind turbine: Pushing the limit of wind turbine technology with complementary design. Applied Energy, 207, 78-95.
[25] Bing Liu, Xinlong Wang, Youle Liu, Yu Gao, Zhun Ma, Jianliang Xue. (2020). Simulation analysis of flow velocity and liquid film of saline wastewater in falling film evaporation. Environmental Technology & Innovation, 19, 100790.
[26] Galindo, J., Fajardo, P., Navarro, R., & García-Cuevas, L. M. (2013). Characterization of a radial turbocharger turbine in pulsating flow by means of CFD and its application to engine modeling. Applied Energy, 103, 116-127.
[27] Chen, J., Yang, H. X., Liu, C. P., Lau, C. H., & Lo, M. (2013). A novel vertical axis water turbine for power generation from water pipelines. Energy, 54, 184-193.
[28] Moffat R J. (1988). Describing the uncertainties in experimental results. Experimental thermal and fluid science, 1(1): 3-17.
[29] Djamal Hissein Didane, Nurhayati Rosly, Mohd Fadhli Zulkafli, Syariful Syafiq Shamsudin. (2019). Numerical investigation of a novel contra-rotating vertical axis wind turbine. Sustainable Energy Technologies and Assessment, 2019, 31, 43-53.

[30] Ying Wang, Xiaojing Sun, Xiaohua Dong, et al. (2016). Numerical investigation on aerodynamic performance of a novel vertical axis wind turbine with adaptive blades. Energy Conversion & Management, 108, 275-286.
[31] S. S. Yang, S. Derakhshan, F. Y. Kong. (2012). Theoretical, numerical and experimental prediction of pump as turbine performance. Renewable energy, 48, 507-513.
[32] Sammartano, V., Filianoti, P., Sinagra, M., Tucciarelli, T., Scelba, G., Morreale, G. (2017) Coupled hydraulic and electronic regulation of cross-flow turbines in hydraulic plants. Journal of Hydraulic Engineering, 143 (1), art. no. 04016071.